Identification and functional assay of an extracellular calcium-sensing receptor in *Necturus* gastric mucosa

ROBERT R. CIMA,[1] IVAN CHENG,[1] MARY E. KLINGENSMITH,[1]
NAIBEDYA CHATTOPADHYAY,[2] OLGA KIFOR,[2] STEVEN C. HEBERT,[3]
EDWARD M. BROWN,[2] AND DAVID I. SOYBEL[1]
[1]*Department of Surgery, West Roxbury Veterans Affairs Medical Center,*
and the [2]*Renal and* [3]*Endocrine-Hypertension Divisions of the Department of Medicine,*
Brigham and Women's Hospital, Harvard Medical School, Boston, Massachusetts 02115

Cima, Robert R., Ivan Cheng, Mary E. Klingensmith, Naibedya Chattopadhyay, Olga Kifor, Steven C. Hebert, Edward M. Brown, and David I. Soybel. Identification and functional assay of an extracellular calcium-sensing receptor in *Necturus* gastric mucosa. *Am. J. Physiol.* 273 (*Gastrointest. Liver Physiol.* 36): G1051–G1060, 1997.—In mammals and amphibians, increases in extracellular Ca^{2+} can activate bicarbonate secretion and other protective functions of gastric mucosa. We hypothesized that the recently cloned extracellular Ca^{2+}-sensing receptor (CaR) is functioning in the gastric mucosa. In *Necturus maculosus* gastric mucosa, reverse transcription-polymerase chain reaction using primers based on previously cloned CaR sequences amplified a 326-bp DNA fragment that had 84% nucleotide sequence identity with the rat kidney CaR. Immunohistochemical localization of the CaR using specific anti-CaR antiserum revealed its presence on the basal aspect of gastric epithelial cells. In microelectrode studies of *Necturus* antral mucosa, exposure to elevated Ca^{2+} (4.8 mM) and the CaR agonists NPS-467 and neomycin sulfate resulted in significant hyperpolarizations of basal membrane electrical potentials and increases in apical-to-basal membrane resistance ratios. Circuit analysis revealed that these changes reflected specific decreases in basolateral membrane resistance. Inhibition of prostaglandin synthesis using indomethacin significantly attenuated these effects. We conclude that the CaR is present and functioning in *Necturus* gastric antrum.

surface epithelium; immunohistochemistry; circuit analysis; electrophysiology

EXTRACELLULAR CALCIUM LEVELS may regulate a variety of epithelial transport mechanisms and mucosal defense properties in the gastric mucosa. Previous studies in mammalian and amphibian models of gastric mucosa have shown that increases in extracellular Ca^{2+} can stimulate both H^+ secretion from the acid-secreting oxyntic glands and HCO_3^- secretion from the neighboring gastric surface epithelium (8, 9, 13, 25). In in vitro studies of gastric surface epithelium in *Necturus maculosus*, we observed marked increases in permeability properties and electromotive forces (EMFs) of the basolateral membranes of the gastric surface cells within 30 s of exposure to increases in Ca^{2+} in the serosal perfusate (20). Circuit analysis and ion substitution protocols indicated that these electrophysiological alterations were attributable to changes in basolateral conductance of K^+ (20). Similar changes in basolateral conductance and potential were elicited by Sr^{2+}, by La^{3+}, and somewhat paradoxically, by high levels (5 mM) of Ba^{2+} in the serosal perfusate. These latter observations suggested that the effects of Ca^{2+} were elicited by its extracellular interactions and not by its passage into the cell interior.

The mechanisms permitting the gastric epithelium to detect and respond to changes in extracellular Ca^{2+} have remained uncharacterized. Recently, however, Brown et al. (3) have cloned and characterized an extracellular Ca^{2+}-sensing receptor (CaR) from bovine parathyroid tissue. This ~120K cell surface receptor, which belongs to the superfamily of G protein-coupled receptors, is activated by changes in the extracellular concentrations of Ca^{2+}, as well as Mg^{2+}, Gd^{3+}, and the polyvalent cation neomycin sulfate. With the use of Northern analysis, the tissue distribution of this receptor was also shown to include mammalian cerebral cortex, cerebellum, thyroid, renal cortex, and renal outer medulla. With the recent identification of this extracellular CaR and its wide tissue distribution, we hypothesized that the CaR may be present and functioning in the gastric mucosa. If so, then it may be responsible for initiating the cellular processes activated by changes in Ca^{2+} levels in the gastric mucosal subepithelial space.

For this study, we used the amphibian *Necturus maculosus* as our model of the gastric mucosa. *Necturus* was chosen because nearly all of the effects of extracellular Ca^{2+} on the transport and permeability properties of the gastric mucosa have been measured in amphibian as well as in mammalian preparations (6, 9, 20). Also, the cellular and epithelial electrophysiological properties of the *Necturus* gastric epithelium have been systematically characterized under a variety of experimental conditions including increases in nutrient Ca^{2+} (2, 10, 20, 22). In this study, we determined whether the CaR was present in the gastric mucosa of *Necturus* by subcloning and sequencing a polymerase chain reaction (PCR) product from the gastric mucosa using CaR-specific primers. In addition, immunohistochemical staining using specific anti-CaR antibodies was used to localize the CaR to the basal surfaces of the epithelium in the *Necturus* gastric mucosa. To determine functional activity of the CaR, we measured the intracellular electrophysiological changes induced in the surface cells in response to various CaR agonists. Intracellular microelectrode techniques were used to perform an equivalent intraepithelial circuit analysis of the antral surface cell in response to a CaR agonist, neomycin sulfate. Finally, interactions with other receptor-activated pathways were explored by evaluating effects of CaR activation after pretreatment with the choliner-

0193-1857/97 $5.00

gic receptor antagonist atropine or the prostaglandin synthesis inhibitor indomethacin.

MATERIALS AND METHODS

Preparation

Necturi (Nasco Biology Division, Ft. Atkinson, WI) were kept in filtered water at 4–8°C. Animals were anesthetized by immersion in oxygenated tank water containing 1% tricaine-methanesulfonate (Sigma Chemical, St. Louis, MO). For Northern analysis and reverse transcription (RT)-PCR, *Necturus* gastric antral and fundic mucosae were harvested by gross dissection and snap frozen in liquid nitrogen and stored at −70°C until further use. Before freezing, the mucosa was rapidly separated from the underlying muscularis by sharp dissection. For in vitro microelectrode studies, tissues were isolated and mounted as described previously (20–23). In brief, antral mucosae were isolated from underlying muscularis and mounted, mucosa side up, in a modified Ussing chamber. The mucosal perfusate (volume 0.5 ml) was continuously exchanged at a rate of 5–7 ml/min. The nutrient perfusate (volume 1.8 ml) was exchanged at a rate of 12–14 ml/min.

RNA Extraction and RT-PCR Analysis

To determine if transcripts for the CaR gene are present in the gastric mucosa of *Necturus*, gastric mucosa RNA was analyzed for expression of this gene product. Total cytoplasmic RNA was extracted from *Necturus* gastric mucosa following the method described previously (3, 5, 14, 19). Briefly, 1 g of tissue was homogenized in 8 ml of a solution containing 4 M guanidine isothiocyanate, 25 mM sodium citrate, and 1.12 g/ml β-mercaptoethanol. The homogenate was layered onto 4 ml of a cushion of 5.7 mM CsCl and 25 mM sodium acetate and spun at 32,000 revolutions/min at 18°C for 18 h. The RNA pellet was resuspended into water and concentrated by precipitation with sodium acetate and ethanol. Total RNA (5 μg) was subjected to single-strand cDNA synthesis in a reaction volume of 20 μl using 25 pmol random hexamer primers, 50 mM tris(hydroxymethyl)aminomethane (Tris)·HCl (pH 8.3), 75 mM KCl, 3 mM $MgCl_2$, 0.5 mM deoxyribonucleotide triphosphates (dNTPs), and 200 U avian myeloblastoma virus reverse transcriptase (Invitrogen, San Diego, CA) at 42°C for 1 h. The resultant first-strand cDNA was used for the PCR reaction. PCR was performed in a total volume of 50 μl in a buffer solution containing 10 mM Tris·HCl, pH 8.3, 50 mM KCl, 1.5 mM $MgCl_2$, 0.25 mM dNTPs, and 10 U of cloned *Pfu* polymerase (Stratagene, La Jolla, CA), using 0.25 nM of sense and antisense primers with the sequences described below. The optimum temperature cycling protocol was determined to be 92°C for 1 min, 55°C for 1 min, and 72°C for 1.5 min for 30 cycles, using a programmable thermal cycler (Omnigene, Hybaid Instruments, Holbrook, NY). The products were then subcloned into the pCR-Script vector (Stratagene) following the supplier's recommendations. The first set of primers was based on a consensus sequence between rat kidney CaR and a partial clone of the *Xenopus* kidney CaR (M. Bei, unpublished observations): 5′-GGACCGAGCCCTTTGGAATCGC-3′, 5′-CGTAGGTGCTGGCATAGGCTGG-3′. RT-PCR performed with this primer pair yielded a PCR product from *Necturus* gastric antrum that was 75% identical in its nucleotide sequence to that of RaKCaR. A second, nested set of primers was then designed based on the sequences of the presumptive gastric *Necturus* RT-PCR product and the *Xenopus* CaR (19): 5′-CTTGACCTCCTTTGTCCTGG-3′, 5′-CGAAGGTGCTCAGAAAGACC-3′. PCR performed with the latter primers yielded the expected 326-bp products from both the gastric fundus and antrum of *Necturus*.

Nucleotide Sequencing of the Clone

Bidirectional sequencing was performed using the dideoxy chain termination method (3, 19) with an Applied Biosystems model 373A automated sequencer (Department of Genetics, Children's Hospital, Boston, MA). Further nucleotide and amino acid analyses were carried out using GeneWorks software (version 2.3.1, IntelliGenetics, Mountain View, CA).

Immunohistochemical Staining

Immunohistochemistry was performed using techniques modified from those described previously (11, 12). Frozen sections were prepared using a cryostat (International Equipment minotome, −20°C) and were postfixed in acetone for 10 min at −20°C.

Endogenous peroxidase inhibition was carried out by incubating the sections in DAKO peroxidase blocking reagent (DAKO, Carpenteria, CA) for 10 min. Nonspecific immunocross-reactivity was blocked by DAKO protein block serum-free solution (DAKO) for 1 h. The sections were then incubated overnight at 4°C with primary (protein A purified) anti-CaR antiserum 4641 at a concentration of 10 μg/ml in blocking solution (DAKO). Characterization of the anti-bovine CaR antibodies has been detailed elsewhere (11, 12, 14). Control sections were prepared by incubation with protein A-purified preimmune serum and with anti-CaR antiserum preabsorbed with the synthetic CaR peptide (amino acids 215–237, 10 μg/ml) against which the antibody was raised. After the sections were washed three times with 0.5% bovine serum albumin in phosphate-buffered saline (PBS) for 20 min each, peroxidase-coupled goat anti-rabbit immunoglobulin G diluted 1:200 (Sigma Chemical) was added and incubated for 1 h at room temperature.

The slides were then washed in PBS three times for 20 min each, and the color reaction was developed using the DAKO AEC substrate system (DAKO) for ~5 min. The color reaction was stopped by washing three times in water. The peroxidase-stained specimens were examined by light microscopy, and photomicrographs were taken at a magnification of ×400 and ×630.

Microelectrode Techniques

Solutions. As previously described, the control solution used as the mucosal and nutrient perfusate during the microelectrode studies is amphibian Ringer solution (106.6 meq/l Na^+, 4.0 meq/l K^+, 1.8 mM Ca^{2+}, 0.8 mM Mg^{2+}, 101.9 mM Cl^-, 13.9 mM HCO_3^-, and 1.0 mM *N*-2-hydroxyethylpiperazine-*N*′-2-ethanesulfonic acid, 5% CO_2-95% O_2 gas) (2, 3, 10, 13). In the elevated Ca^{2+}-Ringer solution, the Ca^{2+} concentration was increased by 3.0 mM to a total Ca^{2+} concentration of 4.8 mM. Solutions of the stereoisomers of the CaR agonist NPS-*R*-467 and NPS-*S*-467 (generously provided by Dr. Edward Nemeth, NPS Pharmaceuticals, Salt Lake City, UT) were prepared to a final concentration of 3.0×10^{-5} M in control Ringer solution ($[Ca^{2+}] = 1.8$ mM) (24). The *R*-isomer of NPS-467 is known to be 100 times more potent as a CaR agonist than the *S*-isomer (24). Neomycin sulfate, another CaR agonist, was used both to measure a dose-response relationship at various nutrient concentrations of neomycin (0.25, 0.5, or 1.0 mM) in a Ringer salt-containing solution ($[Ca^{2+}] = 1.8$ mM) and to perform an intraepithelial circuit analysis. In all subsequent experiments with neomycin, the concentration of neomycin in the nutrient perfusate was 1 mM. All solutions were titrated to pH 7.3. Unless

specifically noted, all reagents used in these experiments were purchased from Sigma Chemical.

Tissue potential and resistance profile. The transepithelial potential (V_{ms}, where m is mucosa and s is serosa) was measured using a high-impedance ($>10^{12}$ Ω) Duo-223 electrometer (World Precision Instruments, Saratoga, FL) providing digital readout. The nutrient solution was grounded, and the mucosal solution was connected to the electrometer by means of a 3.5% agar-Ringer bridge in contact with an Ag/AgCl pellet. Borosilicate glass capillaries were pulled on a two-stage puller (Sutter Instruments, Navato, CA) and backfilled with 3 M KCl. Electrodes with tip potentials and resistances of 15–60 MΩ were used for intracellular impalements. Impalements were obtained using remote-control micromanipulators (Narishige, Tokyo, Japan) on a vibration-free table (Micro G, Woburn, MA). As previously described, criteria for a satisfactory impalement included the following: *1*) an abrupt change in voltage on entry into the cell, *2*) a stable baseline for 60–90 s with a fluctuation of <2 mV while inside the cell, and *3*) a return to the original baseline upon withdrawal of the electrode from the cell (17, 18, 21). The basolateral cell membrane potential (V_{cs}) was measured with reference to the nutrient solution. Apical membrane potential (V_{mc}) was determined from $V_{mc} = V_{cs} - V_{ms}$. All measurements were corrected for junction potentials (17, 18, 21, 22).

Tissue electrical profile and circuit analysis. To measure transepithelial and cell membrane resistances, current pulses of 20 mA and 1-s duration were applied across the mucosa using a Pulsar 4i stimulator (Frederick Haer, Brunswick, ME). Transepithelial resistance (R_T) was determined from the magnitude of the current-induced deflection of the transepithelial potential divided by the current density. The ratio of membrane resistances (R_a/R_b, where R_a is resistance of the apical membrane and R_b that of the basolateral membrane) was determined from the voltage divider ratio (V_{mc}/V_{cs}) as described previously (17, 18, 21). The same experimental protocol was performed for all calculations of tissue potential and resistance profiles (V_{ms}, V_{mc}, V_{cs}, R_T, and R_a/R_b). As previously described, the values of R_a, R_b, and the resistance of the paracellular pathway (R_s) were determined during a brief exposure of the tissue to a mucosal solution containing 10^{-4} M amiloride, a reversible blocker of apical Na^+ conductances in this tissue (17, 21). The assumptions supporting this circuit analysis method have been tested previously and included direct comparison with measurements of the circuit resistances using cable analysis (20, 21).

Values for the EMF generated at the apical (E_a) and basolateral (E_b) cell membrane were calculated as previously described (16, 18, 20). Under control conditions, with both sides of the tissue bathed by identical Ringer solutions, the EMF across the paracellular, or shunt, pathway can be assumed to be 0 mV (18, 20). The apical and basolateral EMFs are then calculated from the following

$$E_a = V_{mc} - V_{ms}(R_a/R_s) \quad (1)$$

$$E_b = V_{cs} + V_{ms}(R_b/R_s) \quad (2)$$

Derivations of these expressions have been given previously (16, 18). These expressions are applicable when ion composition and pH of mucosal and nutrient perfusates are identical.

Experimental Protocols

In all experiments, tissues were mounted and allowed to equilibrate for 30 min, with both sides perfused with control Ringer solution. All tissues were evaluated for changes in potential, resistance, and EMF across individual cell membranes in response to changes in nutrient perfusate composition. In cases where a tissue was sequentially exposed to different agents, there was a recovery period of 30 min, during which both sides were perfused with control Ringer solution. Four series of microelectrode experiments were performed. The first series of experiments quantified the magnitude of electrophysiological changes induced in the surface cell after nutrient exposure to elevated Ca^{2+} or to the stereoisomers of the CaR agonist NPS-467. The second evaluated the dose-response relationship between exposure to the CaR agonist neomycin and electrical profile of the surface cell. In the third series of experiments, a circuit analysis was performed during exposure to neomycin (1 mM) in the nutrient perfusate. At the peak response to neomycin, amiloride (10^{-4} M) was added to the mucosal perfusate, and the circuit analysis was performed. During the last series of experiments, the tissue was incubated with atropine (10^{-4} M) or indomethacin (10^{-4} M) before nutrient neomycin exposure to determine whether the electrophysiological changes induced by CaR activation were altered by pretreatment with these agents.

Data Analysis and Statistical Methods

Data were summarized and analyzed using a standard software statistical package (Excel, Microsoft, Seattle, WA). Results are expressed as means ± SE. Comparisons of paired measurements performed in the same group of tissues were analyzed using an analysis of variance with significance set at $P < 0.05$.

RESULTS

Analysis of CaR Gene Expression

We could not identify specific CaR transcripts in *Necturus* gastric mucosa by Northern analysis, presumably because expression of the CaR was limited to a subset of cells (e.g., see Fig. 2) and the overall level of expression was low. Therefore, 5 μg of total RNA from the gastric antral and fundic mucosa of *Necturus* were subjected to RT-PCR analysis with the two sets of PCR primers described in MATERIALS AND METHODS and yielded similar 326-bp fragments corresponding to a region within the transmembrane domains of the CaR. Nucleic acid sequencing of PCR products from both gastric antrum and fundus revealed 84% identity in their nucleotide sequences with the corresponding region of rat kidney CaR (Fig. 1).

Immunohistochemical Staining

Immunohistochemical staining of the gastric mucosa localized the CaR to the basal surface of the gastric epithelium and in the region of the myenteric plexus. Sections through the fundus revealed minimal staining in the region of the acid-secreting glands. However, staining of antral tissue demonstrated intense staining localized to the basal membrane of the surface cells (Fig. 2). Control sections that were stained with anti-CaR antiserum preabsorbed with the peptide against which it was raised showed no nonspecific binding (Fig. 2). These findings strongly suggest that the CaR is present and localizes predominantly to the basal surface of the gastric epithelium and, in particular, the antral surface cells.

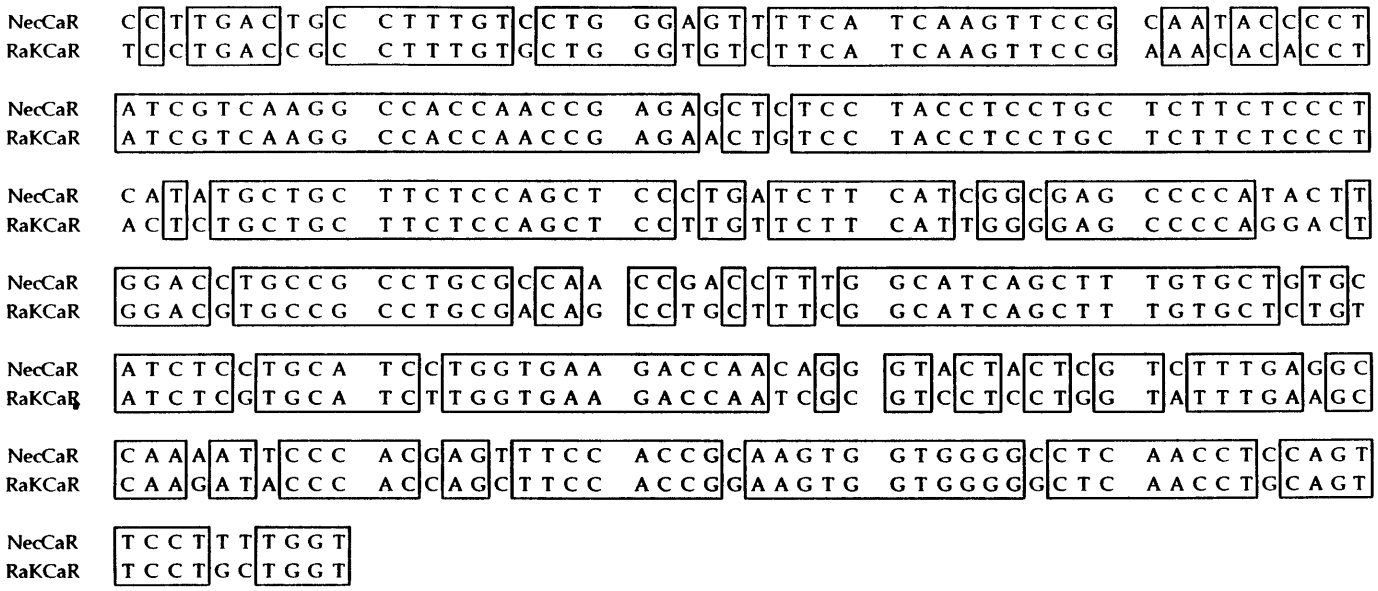

Fig. 1. Nucleotide sequence for *Necturus* 310-bp cDNA fragment (NecCaR) obtained from reverse transcription-polymerase chain reaction of antral mucosa using primers specific for Ca^{2+}-sensing receptor (CaR). Comparison with rat kidney CaR gene (RaKCaR) revealed 84% homology (boxed areas).

Electrophysiological Changes Induced by Elevated Ca^{2+} in the Nutrient Perfusate and NPS-467

Tissues were mounted as described in MATERIALS AND METHODS to evaluate the effects of the stereoisomers of the CaR agonist NPS-467 compared with increased Ca^{2+} in the nutrient perfusate on the electrophysiological properties of the surface cell. After the tissue had equilibrated, the tissue was exposed in random order to either elevated nutrient Ca^{2+}-Ringer solution (total $[Ca^{2+}] = 4.8$ mM) ($n = 13$) or to the *R*-isomer ($n = 10$) or *S*-isomer of NPS-467-Ringer solution ($n = 7$) at a concentration of 3.0×10^{-5} M (total $[Ca^{2+}] = 1.8$ mM). Preliminary studies using NPS-467 in doses ranging from 3.0×10^{-7} to 3.0×10^{-5} M revealed that the most consistent electrophysiological response occurred at 3.0×10^{-5} M. Measurements of the potential difference and resistance profiles for the tissues exposed to elevated nutrient Ca^{2+} and to the stereoisomers of the Ca^{2+} receptor agonist NPS-467 are summarized in Table 1. Elevations of nutrient Ca^{2+} and exposure to the *R*-isomer of NPS-467 elicited significant ($P < 0.05$) and reversible hyperpolarizations of the apical and basal membrane potentials (V_{mc} and V_{cs}, respectively). There was no significant change in the transepithelial electrophysiological properties (V_{ms} or R_T) in response to either elevated Ca^{2+} or to NPS-467. Exposure to either Ca^{2+} or NPS-*R*-467 was accompanied by a significant increase ($P < 0.05$) in the membrane resistance ratio R_a/R_b. Serosal exposure to the *S*-isomer of NPS-467 did not significantly alter cellular or tissue electrical properties.

Electrophysiological Effect of Neomycin in the Nutrient Perfusate

To further investigate the role of CaR activation and associated changes in surface cell electrophysiological properties, surface cell electrical parameters were measured during nutrient exposure to the CaR agonist neomycin. Tissue potential difference and resistance profiles were measured with control Ringer solution ($[Ca^{2+}] = 1.8$ mM) and then during exposure to either 0.25 mM ($n = 10$), 0.5 mM ($n = 10$), or 1 mM ($n = 13$) neomycin ($[Ca^{2+}] = 1.8$ mM) in the nutrient perfusate. A typical tracing of an intracellular recording from a surface cell during exposure to neomycin is shown in Fig. 3. The changes in V_{cs} and R_a/R_b in response to the different concentrations of neomycin in the nutrient perfusate are presented in Fig. 4. The data show that key electrophysiological properties (V_{cs}, R_a/R_b) were altered in a concentration-dependent fashion. As can be seen, at the lower neomycin (0.25 mM) concentration, there was no significant hyperpolarization in V_{cs}. However, as the concentration of neomycin increased (0.5 and 1.0 mM), the magnitude of the hyperpolarization became significant ($P < 0.05$). Similarly, the R_a/R_b increased in a dose-dependent fashion in response to higher concentrations of neomycin ($P < 0.05$). In this instance, even at the lower dose of neomycin there was a small but statistically significant increase in R_a/R_b ($P < 0.05$).

To identify the pathways of ion permeation affected by neomycin exposure, an intraepithelial circuit analysis was performed under control conditions ($[Ca^{2+}] = 1.8$ mM) and during exposure to 1 mM nutrient neomycin ($[Ca^{2+}] = 1.8$ mM) (18). During these experiments, R_a, R_b, and R_s were measured. The apical and basal membrane EMFs were also measured. As previously described, the tissue was exposed to mucosal amiloride (10^{-4} M) Ringer solution either 30 min before or after the nutrient neomycin exposure (18). This amiloride exposure provided an independent measurement of R_a,

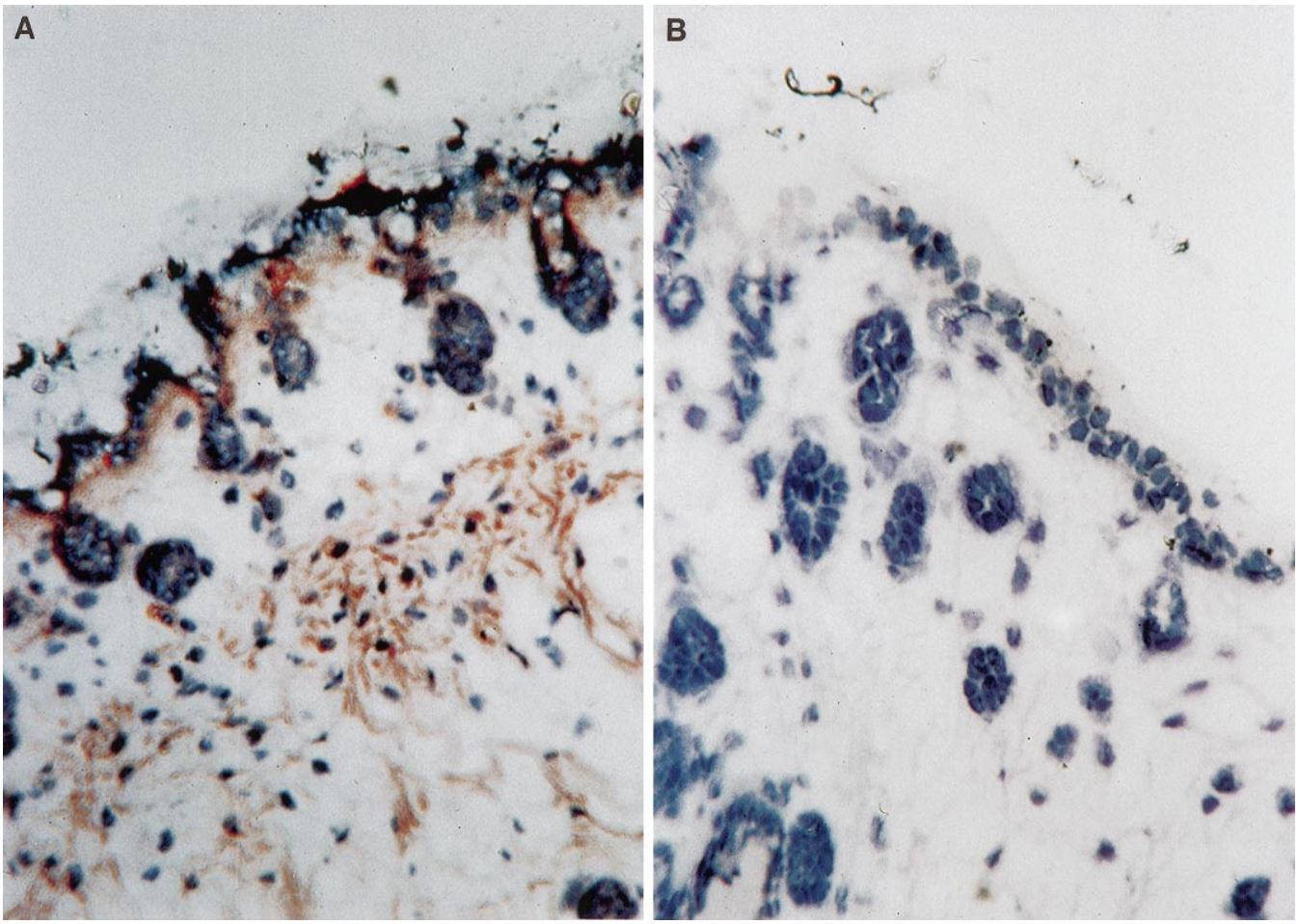

Fig. 2. Immunohistochemical peroxidase staining of full-thickness sections through *Necturus* gastric antrum. *A*: section has been stained with antibodies specific to amphibian CaR. Most intense staining is localized to basal surface of surface epithelium and in myenteric plexus. *B*: section is a nearby control section that has been stained with an anti-amphibian polyclonal immunoglobulin G solution rendered deficient in anti-CaR antibody by immunoabsorbent pretreatment. There is no nonspecific binding observed.

R_b, and R_s. Data from 11 tissues are presented in Table 2. Exposure to nutrient neomycin caused a significant ($P < 0.05$) decrease in the basal membrane resistance (R_b) without affecting the apical membrane (R_a) or paracellular (R_s) resistance. There was also a marked hyperpolarization in E_b ($P < 0.05$). E_a was not significantly altered.

Effect of Atropine and Indomethacin on the Electrophysiological Response to Nutrient Perfusate Neomycin

The final series of studies evaluated possible interactions of CaR activation with other signaling pathways that have been identified in gastric surface epithelium.

Table 1. *Potential and resistance profiles in Necturus antral mucosa during serosal exposure to agonists of the extracellular Ca^{2+}-sensing receptor*

Conditions	*n*	V_{ms}, mV	V_{mc}, mV	V_{cs}, mV	R_T, $\Omega \cdot cm^2$	R_a/R_b
Ringer solution	13	-2.35 ± 0.49	-37.96 ± 1.54	-40.31 ± 1.67	723 ± 72	2.29 ± 0.27
Ringer + 3 mM Ca^{2+}	13	-2.69 ± 0.48	-48.79 ± 1.61*	-51.16 ± 2.31*	724 ± 74	5.51 ± 0.89*
Ringer solution	10	-3.08 ± 0.67	-40.04 ± 2.00	-43.12 ± 1.96	735 ± 93	2.36 ± 0.37
Ringer + 3.0×10^{-5} M NPS-*R*-467	10	-3.33 ± 0.84	-47.28 ± 2.01*	-51.16 ± 2.31*	753 ± 95	4.55 ± 0.87*
Ringer solution	7	-4.71 ± 0.45	-40.84 ± 2.74	-45.56 ± 2.61	826 ± 120	2.07 ± 0.20
Ringer + 3.0×10^{-5} M NPS-*S*-467	7	-4.83 ± 0.48	-44.63 ± 2.33	-49.46 ± 2.30	835 ± 121	2.29 ± 0.15

Values are means ± SE; *n*, no. of tissues. V_{ms}, transepithelial potential; V_{mc}, apical membrane potential; V_{cs}, basolateral membrane potential; R_T, transepithelial resistance; R_a/R_b, ratio of apical to basolateral membrane resistance. *$P < 0.05$ compared with Ringer solution control using analysis of variance.

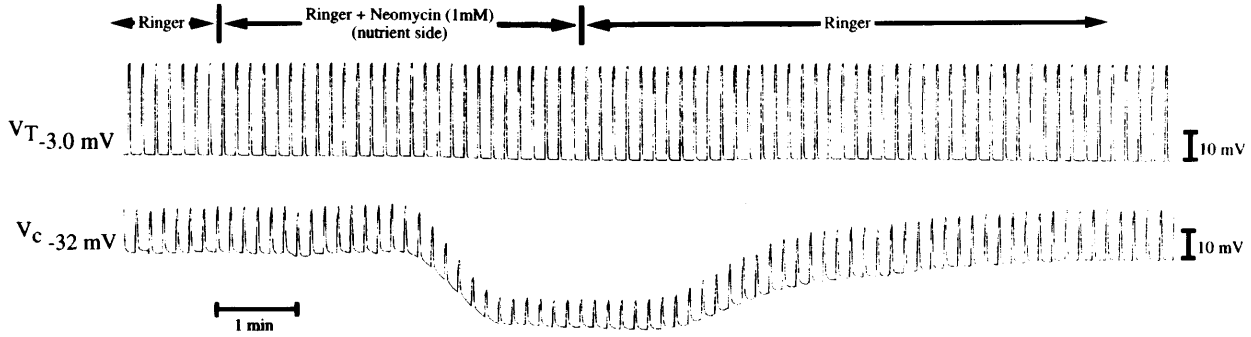

Fig. 3. Effects of nutrient 1 mM neomycin on potential and resistance profile in *Necturus* antral mucosa. V_T, transepithelial potential; V_c, basolateral membrane potential; apical membrane potential ($V_{mc} = V_c - V_T$) not shown. Nutrient solution is reference. Voltage deflections were generated by transepithelial current pulses of 20 μA at 10-s intervals. Recording begins with microelectrode already impaled. Ca^{2+} concentration is held constant at 1.8 mM.

In these studies, cholinergic receptor antagonists and prostaglandin synthesis inhibitors were used before neomycin exposure. Membrane potential differences and resistances were measured in response to 1 mM neomycin after 10 min of exposure to either atropine (10^{-4} M) ($n = 9$) or indomethacin (10^{-4} M) in the nutrient perfusate ($n = 9$). As shown in Fig. 5, atropine had no effect on the hyperpolarization of V_{cs} or on the increase in R_a/R_b resulting from neomycin-induced CaR activation. However, pretreatment of tissues with the prostaglandin synthesis inhibitor indomethacin markedly attenuated the cellular electrophysiological response to CaR activation ($P < 0.05$).

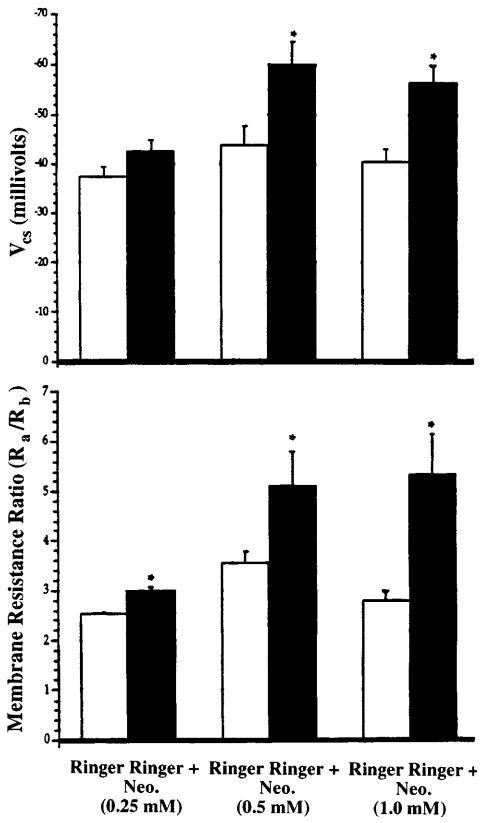

Fig. 4. Summary of effects of progressive increases in nutrient neomycin levels on basolateral membrane potential (V_{cs}) in millivolts and on ratio of cell membrane resistances (R_a/R_b); $n = 10$ for 0.25 and 0.5 mM neomycin (NEO) groups and $n = 14$ for 1 mM neomycin group. *$P < 0.05$ compared with Ringer solution control using an analysis of variance.

DISCUSSION

The principal findings of this study were *1*) detection of a putative CaR by RT-PCR amplification of a fragment resembling rat kidney CaR in the transmembrane domain of the extracellular CaR from the gastric mucosa of *Necturus*; *2*) localization of CaR, using immunohistochemical staining, to the basolateral aspect of the gastric surface epithelium; and *3*) characterization of the electrophysiological response induced in the surface cell due to CaR activation. These findings demonstrate that there is an extracellular CaR present and functionally active in the gastric mucosa of *Necturus*.

Molecular analysis of the gastric mucosa of *Necturus* revealed the presence of a CaR gene product closely homologous to that of the rat CaR (19). Similar to the

Table 2. *Equivalent circuit analysis of changes in potential and resistance profiles in Necturus antral mucosa during exposure to 1 mM nutrient neomycin*

	Ringer Solution	Ringer Solution + 1 mM Neomycin
V_{ms}, mV	−3.47 ± 0.23	−4.52 ± 0.44*
V_{mc}, mV	−34.26 ± 2.00	−50.88 ± 3.56*
V_{cs}, mV	−37.74 ± 2.07	−56.13 ± 3.29*
R_T, Ω·cm^2	672 ± 51	676 ± 48
R_a/R_b	2.63 ± 0.10	5.33 ± 0.69*
R_s, Ω·cm^2	768 ± 90	789 ± 80
R_a, Ω·cm^2	6,618 ± 1,123	6,642 ± 1,993
R_b, Ω·cm^2	2,588 ± 421	1,215 ± 243*
E_a, mV	−0.98 ± 8.18	−14.01 ± 8.17
E_b, mV	−50.79 ± 2.60	−63.07 ± 3.50*

Values are means ± SE, for 11 tissues. V_{ms}, transepithelial potential; V_{mc}, apical membrane potential; V_{cs}, basolateral membrane potential; R_T, transepithelial resistance; R_a/R_b, ratio of apical to basolateral membrane resistance; R_a, R_b, and R_s, resistance of apical membrane, basolateral membrane, and paracellular pathway, respectively; E_a and E_b, apical and basolateral electromotive forces, respectively. *$P < 0.05$ compared with Ringer solution control using an analysis of variance.

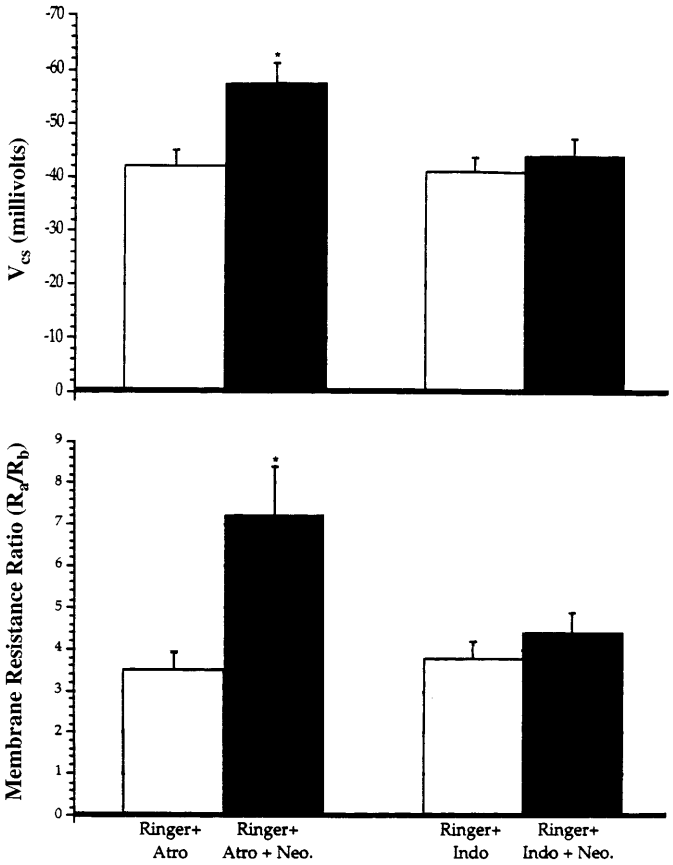

Fig. 5. Summary of effects of preincubation of tissue with atropine (Atro) or indomethacin (Indo) on change in basolateral membrane potential (V_{cs}) and on membrane resistance ratio (R_a/R_b) induced by exposure to 1 mM nutrient neomycin (Neo); $n = 9$ for each experimental group. Atropine and indomethacin were both at a concentration of 10^{-4} M, [Ca^{2+}] = 1.8 mM. *$P < 0.05$ compared with Ringer solution control using an analysis of variance.

work reported by Brown et al. (3) in bovine tissue, we were unable to detect any signal for the CaR from the stomach mucosa using RNA Northern analysis, presumably because of the lower overall level of expression of CaR transcript. However, we were able to identify a fragment of the CaR gene product amplified by RT-PCR. Subsequent immunohistochemical studies localized CaR to the basolateral surface of gastric surface cells and in the region of the myenteric plexus. In this preparation, there was very little staining in the region of the gastric glands. The localization of the CaR to the basal surface of the surface cells is consistent with our finding that Ca^{2+} and the receptor agonists neomycin and NPS-467 elicited their effects when present in the nutrient solution.

The 326-bp PCR product characterized in this study was taken from the highly conserved, transmembrane region of the CaR sequence and was 84% homologous to the corresponding rat sequence (19). This is a slightly higher level of homology than that observed between the chicken and mammalian sequences (7) and not so high as homologies observed between different mammalian species (3, 7, 19). Although the *Xenopus* gene product has not been fully characterized, the degree of homology between the corresponding transmembrane regions is 81% (unpublished observations). Similarly, the extracellular domain of CaR that is recognized by the anti-CaR 4641 antibody has been shown to be highly homologous in avian, amphibian, and mammalian species (3, 7, 19). The high degree of homology in the transmembrane region that was amenable to PCR amplification, taken together with the specificity of antibody staining for a highly homologous extracellular domain of the CaR molecule, indicates that the CaR gene product is highly homologous between *Necturus* and other species. Further characterization of the *Necturus* gene product and its regulatory sites will require development of a cDNA library.

After immunohistochemical localization of the CaR to the basolateral surface of *Necturus* gastric antral cells, our subsequent studies were directed toward demonstrating the electrophysiological responses of the surface epithelium to known CaR agonists. As can be seen from Table 1, increases in nutrient Ca^{2+} result in a marked transient hyperpolarization of both the apical and basolateral membrane potential without a significant change in the transepithelial potential or resistance. There was also a significant increase in R_a/R_b. Thus the current findings with 3.0 mM Ca^{2+} are consistent with our previous findings on the effect of elevated Ca^{2+} in the nutrient perfusate (20). Similar electrophysiological responses of surface cells to specific CaR agonists, such as the NPS-467 compound and neomycin, are strongly suggestive of a receptor-mediated process initiating the observed electrophysiological changes. Also noted in Table 1 are the effects of exposure to the *R*- and *S*-stereoisomers of the CaR agonist NPS-467. These data reveal that the *R*-isomer, which is known to be 100 times more potent than the *S*-isomer, elicits an electrophysiological response nearly identical to that produced by increased Ca^{2+} in the nutrient perfusate (24). The weaker *S*-isomer at the same concentration did not induce these electrophysiological changes. This stereospecific response to the NPS-*R*-467 compound is similar to the CaR activation induced by NPS-467 in bovine parathyroid cells (24). We view this as further evidence that the observed electrophysiological changes in the surface cell are activated through a receptor-mediated process.

To characterize further the electrophysiological response to CaR activation, a number of studies were conducted using the CaR agonist neomycin sulfate. Neomycin was chosen because it has been the best characterized of all of the CaR agonists other than Ca^{2+}, because it is more potent than Ca^{2+}, and because, as a large polyvalent cation, it does not readily cross cell membranes (3). Table 2 shows that, similar to the effects of increased Ca^{2+}, neomycin (1 mM) in the nutrient perfusate caused a significant reversible hyperpolarization of the cell membrane potential and increased the membrane resistance ratio (R_a/R_b). Because exposure to 1 mM neomycin elicited electrophysiological responses similar to those induced by increased

Ca^{2+} in the nutrient perfusate, an intraepithelial circuit analysis using nutrient neomycin was performed to measure the membrane EMFs and determine the pathways of ion permeation affected by neomycin. As presented in Table 2, exposure to neomycin in the nutrient perfusate elicited a significant and marked hyperpolarization restricted to the basolateral membrane EMF and a selective decrease in R_b. There was no significant change in the apical membrane EMF or resistance, nor was there any change in R_s, which is a direct measure of the paracellular pathway resistance. The direction and magnitude of these changes are nearly identical to our previously reported circuit analysis for exposure to 5 mM Ca^{2+} in the nutrient perfusate (20). These findings are highly suggestive that exposure to neomycin in the nutrient perfusate produces the observed electrophysiological effects by a mechanism similar to elevated nutrient Ca^{2+}.

On the basis of the results of the circuit analysis, the effect of CaR activation can be distinguished from the effects of activation of cholinergic or prostaglandin pathways. Both cholinergic and prostaglandin exposure in the nutrient perfusate have been shown to induce significant cell membrane hyperpolarizations and decreases in basolateral resistance in *Necturus* surface cells (1, 10). However, the results of circuit analysis for these compounds have shown that the mechanisms responsible for these changes are quite different from that for Ca^{2+} or neomycin. In our previous circuit analysis for Ca^{2+} exposure in the nutrient perfusate, we showed that the effects of Ca^{2+} on membrane potentials and resistances can be attributed solely to an increase in K^+ conductance across the basolateral membrane (20). This outwardly directed K^+ conductance alone can account for both the hyperpolarization of the basolateral membrane potential and the selective decrease in R_b. In the case of exposure to carbachol (10^{-4} M) in the nutrient perfusate, a cholinergic receptor agonist, there was also a significant hyperpolarization of the basolateral cell membrane potential, as well as a decrease in basolateral membrane resistance (10). However, exposure to carbachol caused no apparent change in the basolateral membrane EMF. This was in contrast to exposure to Ca^{2+} and neomycin, both of which elicited significant hyperpolarizations in the basolateral membrane EMF. Using a circuit analysis such as that performed here, we provided evidence that cholinergic exposure results in activation of both a K^+ and Cl^- conductance across the basolateral membrane (10). With simultaneous activation of a K^+ and Cl^- conductance under baseline conditions, there would be a decrease in R_b because of the increased ion conductance. However, there would be no significant change in E_b under baseline conditions, because E_b is composed of two opposing forces: the hyperpolarizing K^+ conductance and the depolarizing Cl^- conductance. With regard to prostaglandin exposure, the circuit analysis performed by Ashley et al. (1) has shown that, similar to elevated Ca^{2+} and neomycin in the nutrient perfusates, there is hyperpolarization of both the apical and basolateral membrane potentials. However, unlike Ca^{2+} and neomycin, prostaglandin exposure causes a significant decrease in both R_a and R_b as well as an increase in R_s (1). Although the tissue potential and resistance profiles are qualitatively similar for CaR activation and for both cholinergic and prostaglandin stimulation, the circuit analysis indicates that there are clear differences in the mechanisms underlying these electrophysiological changes. Thus we conclude that the electrophysiological changes induced by elevated Ca^{2+} and the CaR agonist neomycin in the nutrient perfusate result from a similar intracellular mechanism, and both are initiated by activation of a basolateral membrane CaR.

Although direct stimulation by either cholinergic receptor agonists or prostaglandins results in different electrophysiological responses in the surface cells, it does not rule out the possibility that either of these major intraepithelial signaling pathways may influence the efficacy or ability of the CaR to cause the observed electrophysiological response. As shown in Fig. 5, atropine, which is a nonselective muscarinic receptor antagonist, does not alter the electrophysiological response induced by neomycin exposure. However, indomethacin, which inhibits prostaglandin synthesis, markedly attenuates the response. These data suggest that the signaling pathway that links the activation of the CaR to the activation of the K^+ conductance is dependent on prostaglandin synthesis. Further experiments are required to better define the relationship between activation of the CaR and activation of the basolateral membrane K^+ conductance.

In summary, we have reported evidence for the presence of a functionally active extracellular CaR in the basal membrane of the gastric mucosa of *Necturus*. We have identified the presence of the CaR in the gastric mucosa by *1*) using RT-PCR to amplify and then sequence a fragment of the CaR gene from the gastric mucosa, and *2*) localizing the CaR to the basal membrane of the gastric antral surface cells by immunohistochemical staining. Intracellular microelectrode techniques were used to measure an electrophysiological response of the surface cell to activation of the CaR. The intracellular hyperpolarization and selective increase in basal membrane conductance in response to CaR activation by increased Ca^{2+} and known CaR agonists such as the NPS-467 compound and neomycin in the nutrient perfusate provide evidence that this is a receptor-mediated process. The stereospecific response to the *R*-isomer of the NPS-467 CaR agonist as opposed to the *S*-isomer is further suggestive of a receptor-mediated process.

Although we have presented evidence for the existence of a functionally active extracellular CaR in the basal surface of *Necturus* gastric mucosa, we have not demonstrated a physiological role for the CaR in the gastric mucosa. In this regard, it should be noted that, across several species, CaR sequences have now been identified not only in tissues that regulate Ca^{2+} homeostasis, such as parathyroid, thyroid C cells, and kidney, but also in tissues of the central and peripheral auto-

nomic nervous systems (4), as well as endocrine cells such as the gastrin-secreting G cells of gastric antral mucosa (15). Thus CaR is not localized only in tissues that contribute directly to absorption or excretion of Ca^{2+}.

In such tissues, one possible function of the CaR may be to communicate the level of Ca^{2+} in the extracellular microenvironment, which may in turn alter intracellular processes. Changes in the microenvironment that may occur during periods of acid or bicarbonate secretion may change the level of ionized Ca^{2+}, and thus the CaR may serve as a mechanism to regulate these processes. Alternatively, the Ca^{2+} concentration in this microenvironment may increase during injury to the epithelium, and thus the CaR may serve to sense these changes in Ca^{2+} and then activate cellular defense mechanisms. The suggestion that inhibitors of prostaglandin synthesis may interfere with one of the signaling mechanisms affected by activation of the CaR is interesting considering the role of prostaglandins in maintaining the integrity of the gastric mucosa. With the evidence that we have presented in regard to the presence of the CaR in the gastric surface epithelium, a role for Ca^{2+} as a true first messenger may be postulated. Further studies are needed to elucidate the exact role of the CaR in the gastric mucosa and to determine what role this receptor may play, if any, in maintaining the integrity of the gastric mucosa.

This work was supported by National Institute of Diabetes and Digestive and Kidney Diseases Grants DK-09288-02 (to R. R. Cima), DK-09033 (to M. E. Klingensmith), and DK-44571-02 (to D. I. Soybel); Howard Hughes Medical Institute Research Training Fellowship for Medical Students (to I. Cheng); and I-S R- & S-467 individual and NPS Pharmaceutical Grants DK-41415 and DK-48330 (to E. M. Brown).

Portions of this work have been presented in abstract form at the Fundamental Forum, American College of Surgeons Meeting (San Francisco, CA, October 1996) and Digestive Diseases Week (Washington, DC, May 1997).

Address for reprint requests: D. I. Soybel, Dept. of Surgery/112, West Roxbury Veterans Administration Medical Center, 1400 VFW Parkway, West Roxbury, MA 02132.

Received 13 May 1997; accepted in final form 18 August 1997.

REFERENCES

1. **Ashley, S. W., D. I. Soybel, and L. Y. Cheung.** Effect of 16,16-dimethyl prostaglandin E_2 on gastric epithelial cell membrane potentials and resistances. *Surgery* 98: 166–172, 1985.
2. **Ashley, S. W., D. I. Soybel, L. De, and L. Y. Cheung.** Microelectrode studies of *Necturus* antral mucosa. II. Equivalent circuit analysis. *Am. J. Physiol.* 248 (*Gastrointest. Liver Physiol.* 11): G574–G579, 1985.
3. **Brown, E. M., G. Gamba, D. Riccardi, M. Lombardi, R. Butters, O. Kifor, A. Sun, M. A. Hediger, J. Lytton, and S. C. Hebert.** Cloning and characterization of an extracellular Ca^{2+}-sensing receptor from bovine parathyroid. *Nature* 366: 575–580, 1993.
4. **Cheng, I., O. Kifor, N. Chattopadhyay, R. R. Butters, R. R. Cima, S. C. Hebert, E. M. Brown, and D. I. Soybel.** Expression of an extracellular Ca^{2+}-sensing receptor in rat gastrointestinal tract (Abstract). *Gastroenterology* 112: A1139, 1997.
5. **Chirgwin, J. M., A. E. Przybyla, R. J. MacDonald, and W. J. Rutter.** Isolation of biologically active ribonucleic acid from sources enriched in ribonuclease. *Biochemistry* 18: 5294–5299, 1979.
6. **Critchlow, J., D. Magee, S. Ito, K. Takeuchi, and W. Silen.** Requirement for restitution of the surface epithelium of frog stomach after mucosal injury. *Gastroenterology* 88: 237–249, 1985.
7. **Diaz, R., S. Hurwitz, N. Chattopadhyay, M. Pines, Y.-H. Yang, O. Kifor, M. S. Einat, R. Butters, S. C. Hebert, and E. M. Brown.** Cloning, expression, and tissue localization of the calcium-sensing receptor in chicken (*Gallus domesticus*). *Am. J. Physiol.* 273 (*Regulatory Integrative Comp. Physiol.* 42): R1008–R1016, 1997.
8. **Flemström, G.** Effects of catecholamines, Ca^{2+} and gastrin on gastric HCO_3^- secretion. *Acta Physiol. Scand.* 88, *Suppl.*: 81–90, 1978.
9. **Flemström, G., and A. Garner.** Stimulation of gastric acid and bicarbonate secretions by calcium in guinea pig stomach and amphibian isolated mucosa. *Acta Physiol Scand.* 110: 419–426, 1980.
10. **Gadacz, A. E., M. E. Klingensmith, and D. I. Soybel.** Electrophysiological effects of cholinergic agonists in surface epithelium of *Necturus* gastric antrum. *Am. J. Physiol.* 270 (*Gastrointest. Liver Physiol.* 33): G449–G462, 1996.
11. **Ho, C., D. A. Conner, M. Pollak, D. J. Ladd, O. Kifor, H. Warren, E. M. Brown, C. E. Seidman, and J. G. Seidman.** A mouse model for familial hypocalciuric hypercalcemia and neonatal severe hyperparathyroidism. *Nature Genet.* 11: 389–394, 1995.
12. **Kifor, O., F. D. Moore, Jr., P. Wang, M. Goldstein, P. Vassilev, I. Kifor, S. C. Hebert, and E. M. Brown.** Reduced immunostaining for the extracellular Ca^{2+}-sensing receptor in primary and uremic secondary hyperparathyroidism. *J. Clin. Endocrinol. Metab.* 81: 1598–1606, 1996.
13. **Main, H. M., and J. B. Pearce.** Effect of calcium on acid secretion from the rat isolated gastric mucosa during stimulation with histamine, pentagastrin, methacholine, and dibutyryl cyclic adenosine-3′,5′-monophosphate. *Br. J. Pharmacol.* 64: 359–368, 1978.
14. **Mithal, A., O. Kifor, I. Kifor, P. Vassilev, R. Butters, K. Krapcho, R. Simin, F. Fuller, S. C. Hebert, and E. M. Brown.** The reduced responsiveness of cultured bovine parathyroid cells to extracellular Ca^{2+} is associated with marked reduction in the expression of extracellular Ca^{2+}-sensing receptor mRNA and protein. *Endocrinology* 136: 3087–3092, 1995.
15. **Ray, J. M., P. E. Squires, S. B. Curtis, M. R. Meloche, and A. M. J. Buchan.** Expression of the calcium-sensing receptor on human antral gastrin cells in culture. *J. Clin. Invest.* 10: 1–8, 1997.
16. **Reuss, L.** Electrical properties of the cellular transport pathway in *Necturus* gallbladder. III. Ionic permeability of the basolateral membrane. *J. Membr. Biol.* 47: 239–259, 1979.
17. **Reuss, L., and A. L. Finn.** Passive electrical properties of toad urinary bladder epithelium: intercellular coupling and transepithelial cellular and shunt conductances. *J. Gen. Physiol.* 64: 1–25, 1974.
18. **Reuss, L., and A. L. Finn.** Electrical properties of the cellular transepithelial pathway in *Necturus* gallbladder. I. Circuit analysis and steady-state effects of mucosal ionic substitutions. *J. Membr. Biol.* 25: 115–139, 1975.
19. **Riccardi, D., J. Park, L. Wen-Sen, G. Gamba, E. M. Brown, and S. C. Hebert.** Cloning and functional expression of a rat kidney extracellular calcium/polyvalent cation-sensing receptor. *Proc. Natl. Acad. Sci. USA* 92: 131–135, 1995.
20. **Soybel, D. I., S. W. Ashley, and L. Y. Cheung.** Basolateral K^+ conductances in surface epithelium of *Necturus* antrum: effects of Ca^{2+} and divalent cations. *Am. J. Physiol.* 262 (*Gastrointest. Liver Physiol.* 25): G651–G659, 1992.
21. **Soybel, D. I., S. W. Ashley, R. A. Swarm, C. D. Moore, and L. Y. Cheung.** Effects of luminal salt concentration on electrical pathways in *Necturus* antrum. *Am. J. Physiol.* 252 (*Gastrointest. Liver Physiol.* 15): G19–G27, 1987.
22. **Soybel, D. I., M. B. E. Davis, and L. Y. Cheung.** Characteristics of basolateral Cl^- transport in *Necturus* antral mucosa. *Am. J. Physiol.* 264 (*Gastrointest. Liver Physiol.* 27): G910–G920, 1993.

23. **Soybel, D. I., M. B. E. Davis, and A. B. West.** Effects of aspirin on pathways of ion permeation in *Necturus* antrum: role of nutrient HCO_3^-. *Gastroenterology* 103: 1475–1485, 1992.
24. **Steffey, M. E., J. Fox, B. C. VanWagenen, E. G. Delmar, M. F. Balandrin, and E. F. Nemeth.** Calcimimetics: structurally and mechanistically novel compounds that inhibit hormone secretion from parathyroid cells (Abstract). *J. Bone Miner. Res.* 8, *Suppl*. 1: S175, 1993.
25. **Walker, W., A. Vinik, A. Heldsinger, and R. Kaveh.** Role of calcium and calmodulin in activation of the oxyntic cell by histamine and carbamylcholine in the guinea pig. *J. Clin. Invest.* 72: 955–964, 1983.